











ORIGINAL RESEARCH

Assessment of an ECG-Based System for Localizing Ventricular Arrhythmias in Patients With Structural Heart Disease

Shijie Zhou , PhD; Amir AbdelWahab , MD; John L. Sapp , MD; Eric Sung , BA; Konstantinos N. Aronis , MD; James W. Warren, BSc; Paul J. MacInnis, BSc; Rushil Shah , MBBS, MHS; B. Milan Horáček, PhD; Ronald Berger , MD, PhD; Harikrishna Tandri , MD; Natalia A. Trayanova , PhD*; Jonathan Chrispin , MD*

BACKGROUND: We have previously developed an intraprocedural automatic arrhythmia-origin localization (AAOL) system to identify idiopathic ventricular arrhythmia origins in real time using a 3-lead ECG. The objective was to assess the localization accuracy of ventricular tachycardia (VT) exit and premature ventricular contraction (PVC) origin sites in patients with structural heart disease using the AAOL system.

METHODS AND RESULTS: In retrospective and prospective case series studies, a total of 42 patients who underwent VT/PVC ablation in the setting of structural heart disease were recruited at 2 different centers. The AAOL system combines 120-ms QRS integrals of 3 leads (III, V2, V6) with pace mapping to predict VT exit/PVC origin site and projects that site onto the patient-specific electroanatomic mapping surface. VT exit/PVC origin sites were clinically identified by activation mapping and/or pace mapping. The localization error of the VT exit/PVC origin site was assessed by the distance between the clinically identified site and the estimated site. In the retrospective study of 19 patients with structural heart disease, the AAOL system achieved a mean localization accuracy of 6.5 ± 2.6 mm for 25 induced VTs. In the prospective study with 23 patients, mean localization accuracy was 5.9 ± 2.6 mm for 26 VT exit and PVC origin sites. There was no difference in mean localization error in epicardial sites compared with endocardial sites using the AAOL system (6.0 versus 5.8 mm, $P=0.895$).

CONCLUSIONS: The AAOL system achieved accurate localization of VT exit/PVC origin sites in patients with structural heart disease; its performance is superior to current systems, and thus, it promises to have potential clinical utility.

Key Words: ECG ■ pace-mapping ■ premature ventricular contraction (PVC) ■ radiofrequency (RF) ablation ■ structural heart disease (SHD) ■ ventricular tachycardia (VT)

Catheter ablation is an established therapeutic option for ventricular tachycardias (VTs) or premature ventricular contractions (PVCs) in patients with structural heart disease (SHD).¹ Localizing the VT exit site or the PVC origin site can be critical for successful VT catheter ablation in these patients.² In 2012, Yokokawa et al first demonstrated the feasibility of using a computerized algorithm based on ECG morphologies of known pacing sites to localize a scar-related VT

exit site using the 12-lead ECG.³ However, the algorithm had a resolution of one of 10 segments of the left ventricular (LV) endocardial surface. To achieve higher precision, a population-derived regression approach to localize the site of origin of early LV activation onto one of 238 triangular area elements of a generic LV endocardial surface was developed,^{4,5} achieving a mean localization accuracy of 9.5 ± 2.6 mm in a prospective validation study.⁶

Correspondence to: Shijie Zhou, PhD, Alliance for Cardiovascular Diagnostic and Treatment Innovation, Johns Hopkins University, Hackerman Hall, Suite 218, 3400 North Charles Street, Baltimore MD, 21218. E-mail: shijie.zhou@jhu.edu

*N. A. Trayanova and J. Chrispin are co-primary investigators and co-senior authors.

For Sources of Funding and Disclosures, see page 12.

© 2021 The Authors. Published on behalf of the American Heart Association, Inc., by Wiley. This is an open access article under the terms of the Creative Commons Attribution-NonCommercial-NoDerivs License, which permits use and distribution in any medium, provided the original work is properly cited, the use is non-commercial and no modifications or adaptations are made.

JAHA is available at: www.ahajournals.org/journal/jaha

CLINICAL PERSPECTIVE

What Is New?

- In patients with structural heart disease, the automatic arrhythmia-origin localization system identified ventricular tachycardia exit sites and premature ventricular contraction sites of origin onto an electroanatomic map in real-time using a 3-lead ECG, with a mean localization error of 6.5 mm in a retrospective case series study and 5.9 mm in a prospective study.
- The localization error for the automatic arrhythmia-origin localization system in patients with structural heart disease is the smallest currently reported for an ECG-based localization algorithm.
- The automatic arrhythmia-origin localization system can accurately localize ventricular tachycardia exit/premature ventricular contraction origin sites on the epicardial and endocardial electroanatomic mapping surfaces.

What Are the Clinical Implications?

- The intraprocedural automatic arrhythmia-origin localization system, which can accurately localize a ventricular tachycardia exit/premature ventricular contraction origin site, can potentially reduce the time needed for detailed mapping by quickly identifying a focused region of interest.

Nonstandard Abbreviations and Acronyms

AAOL	automatic arrhythmia origin localization
EAM	electroanatomic mapping
PVC	premature ventricular contraction
SHD	structural heart disease

Recently, we have developed an automatic arrhythmia origin localization (AAOL) system⁷ which does not require a complete electroanatomic mapping (EAM) for localization of the origin of focal ventricular arrhythmias on a patient-specific geometry of the LV, the right ventricle and neighboring vessels. The AAOL system, which combines 3-lead ECG (leads III, V2, V6) with pace mapping to predict the ventricular arrhythmia origin on the patient-specific EAM surface created at the discretion of the operating electrophysiologist, was shown in a prospective multicenter study to achieve a mean localization error of 3.6 mm.⁷ However, the AAOL system localization performance has not been validated in patients with SHD. This study has 2 objectives: (1) to demonstrate the feasibility of the AAOL

system for localizing the VT exit/PVC origin site in patients with SHD, and (2) to quantitatively estimate the localization accuracy of the AAOL system in identifying the VT exit/PVC origin site in both the epicardial and endocardial ventricular surface.

METHODS

Data Availability

Data are available from the corresponding author on reasonable request. Requests for the data may be sent to the corresponding author at shijie.zhou@jhu.edu.

Study Population

Patients who underwent VT/PVC ablation for SHD at 2 different centers were enrolled in the study. A retrospective case series study composed of 19 patients enrolled by the Queen Elizabeth II Health Sciences Centre, as has been previously described.⁶ A prospective case series study included 23 patients from the Johns Hopkins Hospital. The study protocol was reviewed and approved by the institutional review boards of the participating institutions. Written informed consent was obtained from all patients to participate in the study.

Clinical Electrophysiology Mapping

The VT ablation procedure was performed using standard techniques,⁸ or infusion-needle catheter ablation.⁹ Use of the needle catheter was conducted through the Special Access Program, Health Canada. Access to the LV was achieved via a retrograde aortic or trans-septal approach, and to the right ventricle via a transvenous approach. Epicardial catheter mapping and ablation of VT was performed as previously described.^{10,11} VT was induced by programmed ventricular stimulation from the right ventricular (RV) apex, RV outflow tract or LV. For each procedure, intracardiac electrograms were digitized and stored by CardioLab system (GE Healthcare, Barrington, Illinois). Carto 3 (Biosense Webster, Diamond Bar, CA) or EnSite Precision (Abbott, St. Paul, MN) mapping system was used for EAM. An EAM was created using an open-irrigated catheter (ThermoCool SmartTouch., Biosense Webster, Diamond Bar, CA; FlexAbility SE, Abbott, Abbott Park, IL) or a high-density (HD) multi-electrode catheter (PentaRay NAV Catheter, Biosense Webster; Grid Catheter, Abbott, Abbott Park, IL). The use of the image integration module (CartoSound, Biosense Webster, Diamond Bar, CA) was left to the discretion of the attending electrophysiologist. Activation and entrainment mapping was performed for hemodynamically stable VT, per established criteria.¹² For hemodynamically

unstable VT, substrate-based mapping targeting local abnormal ventricular activity and late potentials along with pace mapping were used to identify culprit sites within areas of scar, which were targeted for ablation, giving particular attention to substrate proximal to VT exit sites. Pacing-site distribution was at the discretion of the operating electrophysiologist. Pacing was performed with a stable catheter position at multiple sites at minimum pacing output (range: 1 milliamp [mA] to 10 mA) which ensured consistent focal myocardial capture, at which point the Carto 3/EnSite Precision mapping system was used to tag it and acquire the x , y , z coordinates.

AAOL System

Standard 12-lead ECGs of induced VTs or paced beats were acquired via the CardioLab system (GE Healthcare, Waukesha, WI) during the ablation procedure. The analog output of the amplifier and system which routinely processes the signal was digitized using an A/D converter (National Instruments, Austin, TX); simultaneously, the digital signal was cloned to an ancillary secured computer where additional processing and analysis can be performed by the AAOL system without affecting the clinical signal. The ECGs of the induced VT and the paced beats were recorded in real time. Currently, given the fact that the system is not integrated with a commercial mapping system, it takes 2 to 3 minutes to transfer the 3-dimensional coordinates of the pacing sites and the EAM geometries to the ancillary secured computer with the AAOL system.

A complete description of the AAOL can be found in our previous publication.⁷ For each procedure, we used all recorded pacing sites of VTs/PVCs being mapped to assess the localization performance of the AAOL system. Briefly, for each recorded pacing site the coordinate of the EAM geometry and their corresponding 3-lead ECGs (leads III, V2, V6) were used to compute patient-specific regression coefficients in a multiple regression model. To localize an induced VT/PVC, the AAOL system determines the 120-ms QRS integrals of 3 leads of the induced VT/PVC and uses the calculated patient-specific regression coefficients to predict the VT exit/PVC origin site coordinates (x , y , z). The predicted VT exit/PVC origin site coordinates (x , y , z) are projected onto the EAM surface mesh using a nearest neighbor algorithm, so that the location can be targeted as a predicted VT exit/PVC origin site. For a procedure with multiple VTs/PVCs, the AAOL system uses the same patient-specific regression coefficients calculated from all recorded pacing sites to identify the VT exit/PVC origin sites.

Statistical Analysis

Localization of a pacing site or an induced VT/PVC was performed on an ancillary secured computer

with the AAOL system. For a recorded pacing site, 1 representative paced beat was selected in the corresponding 12-lead ECG, avoiding ectopic beats, motion artifacts, non-capture beats, and captured beats with stimulus-QRS delay >40 ms (as these may represent capture of a channel within myocardial scar with exit remote from the site of pacing). Localization errors were quantitatively estimated by 1 investigator who was masked to the results of the VT ablation procedure.

Estimation of Localization Accuracy of the Pacing Site Using the AAOL in Patients With SHD

We used recorded pacing sites to estimate the localization accuracy of the AAOL system for each patient. Each pacing site was identified as a target site; the remaining pacing sites were used to calculate patient-specific regression coefficients by combining their known sites and ECG integrals from leads III, V2, and V6. The patient-specific regression coefficients and the 3-lead 120-ms QRS integrals of the target site were then used to estimate the location of the target site. Accuracy was calculated as the distance between the estimated sites and actual pacing sites projected onto the patient-specific EAM surface.

Table 1. Baseline Characteristics of the Retrospective and Prospective Case Series Studies

Clinical characteristics	Retrospective case series (n=19)	Prospective case series (n=23)
Men (%)	17 (89.5)	21 (91.3)
Age, y	66.6±9.1	62.7±18.3
Non-ischemic	3 (15.8)	3 (13.0)
Ischemic cardiomyopathy	15 (79.0)	13 (56.5)
Cardiac sarcoid	1 (5.3)	1 (4.4)
ARVD/ARVC	...	6 (26.1)
LVEF (%)	37.8	34.8
Heart failure (%)	14 (73.7)	14 (60.8)
ICD present	15 (78.9)	20 (87.0)
CRT-D present	2 (10.5)	3 (13.0)
Medication (%)		
Beta blocker	13 (68.4)	20 (87.0)
Amiodarone	10 (52.6)	10 (43.5)
Mexiletine	4 (21.1)	2 (8.7)

ACEi indicates angiotensin-converting enzyme inhibitors; ARVD/ARVC, arrhythmogenic right ventricular dysplasia/arrhythmogenic right ventricular cardiomyopathy; CRT-D, cardiac resynchronization therapy defibrillator; ICD, implantable cardioverter defibrillator; LVEF, left ventricular ejection fraction; and VT, ventricular tachycardia.

Table 2. Description of All Recorded VTs and PVCs From the Prospective Case Series Study

Case #	Sex	Age, y	Etiology	Epi/Endo Procedure	VT	Characteristics of VT morphology
1	M	73.8	ICM	Endo	VT1	RB/Indeterminate axis/Tran V ₅ -V ₆ /CL 520 ms
2	M	80.1	NICM	Endo and Epi	VT1	RB/Inferior axis/Positive V ₁ -V ₆ /CL 500 ms
					VT2	RB/Superior axis/Tran V ₄ /CL 425 ms
3	M	43.4	ARVC	Epi and Endo	PVC1	LB/Superior axis/Negative V ₁ -V ₆ /NA
					PVC2	LB/Inferior axis/Tran V ₃ /NA
					PVC3	LB/Superior axis/Tran V ₄ /NA
4	M	63.1	ARVD	Epi	VT1	RB/Inferior axis/Positive V ₁ -V ₆ /CL 367 ms
5	M	77.0	ICM	Endo	VT1	RB/Indeterminate axis/Tran V ₂ /CL 551 ms
6	M	76.8	ICM	Endo	VT1	RB/Indeterminate axis/Tran V ₄ -V ₅ /CL 523 ms
					VT2	RB/Superior axis/Tran V ₄ /CL 423 ms
					VT3	RB/Superior axis/Tran V ₅ -V ₆ /CL 408 ms
7	M	81.2	ICM	Endo	VT1	LB/Superior axis/Trans V ₃ /CL 420 ms
					VT2	RB/Superior axis/Trans V ₂ -V ₃ /CL 270 ms
8	M	72.9	ICM	Endo	VT1	RB/Superior axis/Positive V ₁ -V ₆ /CL 528 ms
					VT2	LB/Superior axis/Trans V ₄ -V ₅ /CL 438 ms
					VT3	RB/Superior axis/Trans V ₃ /CL 474 ms
9	M	73.9	ICM	Endo	VT1	LB/Indeterminate axis/Tran V ₂ /CL 241 ms
					VT2	RB/Indeterminate axis/Tran V ₄ -V ₅ /CL 303 ms
10	M	64.6	ICM	Endo	VT1	LB/Inferior axis/Tran V ₅ /CL 360 ms
11	M	53.0	NICM	Endo	VT1	RB/Superior axis/Tran V ₂ -V ₃ /CL 341 ms
					VT2	LB/Inferior axis/Tran V ₂ -V ₃ /CL 299 ms
					VT3	RB/Superior axis/Tran V ₂ -V ₃ /CL 299 ms
12	M	24.2	ARVC	Epi	...	No-inducible VT
13	M	69.3	ICM	Endo	VT1	LB/Inferior axis/Tran V ₃ /CL 281 ms
14	M	52.6	ARVC	Epi and Endo	PVC1	LB/Inferior axis/Tran V ₃ -V ₄ /NA
15	M	73.7	NICM	LV Endo	VT1	LB/Inferior axis/Tran V ₃ /460 ms
					VT2	RB/Inferior axis/Positive V ₁ -V ₆ /460 ms
					VT3	RB/Indeterminate axis/Positive V ₁ -V ₆ /490 ms
16	M	25.6	ICM	Endo	VT1	LB/Superior axis/qs in V ₁ , biphasic in V ₂ -V ₃ , and negative in V ₄ -V ₆ /280 ms
					VT2	RB/Superior axis/Tran V ₄ -V ₅ /CL 270 ms
					VT3	LB/Indeterminate axis/ Tran V ₃ -V ₄ /CL 400 ms
17	M	62.0	ICM	Endo	VT1	RB/Superior axis/Tran V ₂ /CL 370 ms
					VT2	RB/Inferior axis/Positive V ₁ -V ₆ /CL 330 ms
					VT3	RB/Superior axis/Tran V ₃ /CL 280 ms
18	F	22.2	ARVC	Epi and Endo	PVC1	LB/Inferior axis/Tran V ₃ /NA
					PVC2	RB/Superior axis/Negative V ₁ -V ₆ /NA
19	F	59.3	ARVC	Epi and Endo	VT1	LB/Superior axis/Negative V ₁ -V ₆ /CL 318 ms
					VT2	LB/Indeterminate axis/Tran V ₆ /CL 363 ms
					VT3	LB/Inferior axis/Tran V ₆ /CL 258 ms
20	M	61.4	CS	Endo	VT1	LB/Inferior axis/Tran V ₄ /CL 270 ms
					VT2	RB/Inferior axis/Positive V ₁ -V ₆ /CL 260 ms
					VT3	LB/Indeterminate axis/Tran V ₂ -V ₃ /CL 292
					VT4	RB/Superior axis/Tran V ₆ /CL 249 ms
					VT5	RB/Superior axis/Tran V ₅ /CL 299ms
					VT6	RB/Superior axis/Positive V ₁ -V ₆ /CL 226 ms

(Continued)

Table 2. Continued

Case #	Sex	Age, y	Etiology	Epi/Endo Procedure	VT	Characteristics of VT morphology
21	M	74.9	ICM	Endo	VT1	RB/Indeterminate axis/Tran V ₄ /CL 460 ms
					VT2	RB/Inferior axis/Tran V ₄ /CL 335 ms
22	M	82.8	ICM	Epi	VT1	RB/Indeterminate axis/Tran V ₂ /CL 400 ms
23	M	74.1	ICM	Endo	VT1	LB/Inferior axis/Tran V ₆ /CL 393 ms
					VT2	RB/Superior axis/Positive V ₁ -V ₆ /CL 326 ms

Description of ventricular tachycardia morphology: ventricular tachycardia morphology/axis based on 3 leads (inferior axis (positive in II, III, augmented Vector Foot leads), Superior axis (negative in II, III, augmented Vector Foot leads), Indeterminate axis)/QRS transition zone/cycle length; NA indicates that the cycle length was not definitely identified.

ARVC, arrhythmogenic right ventricular cardiomyopathy; ARVD, arrhythmogenic right ventricular dysplasia; aVF, augmented Vector Foot; CL, cycle length; CS, cardiac sarcoid; Endo, endocardial ablation procedure; Epi, epicardial ablation procedure; ICM, ischemic cardiomyopathy; LB, left bundle; LV, left ventricular; M, male; F, female; NICM, non-ischemic cardiomyopathy; PVC, premature ventricular contraction; RB, right bundle; RV, right ventricular; and VT, ventricular tachycardia.

Estimation of Localization Accuracy of the VT Exit/PVC Origin Site Using the AAOL in Patients With SHD

All VT ablation procedures for SHD were performed by clinicians masked to the prediction results of the AAOL system. The VT exit/PVC origin site was clinically identified and confirmed by a combination of activation mapping¹³ and entrainment mapping during VT,¹⁴ supplemented by pace mapping at the scar margin.^{15,16} Locations were defined as exit sites if:

1. Entrainment resulted in concealed fusion with a difference of <30 msec between post-pacing interval and tachycardia cycle length, and if stimulus-QRS interval and electrogram-QRS interval was <40 msec; or
2. Local activation time during VT was 0–40 msec pre-QRS; or
3. A conducting corridor was identified within scar at which pacing resulted in >40 msec latency and >95% quantitative morphologic match and further mapping identified a site at or near the scar margin with <40 msec latency but preserved morphology match.

Induced VTs/PVCs for which an accurate scar exit site were not verifiable by contact mapping methods were excluded. Estimated localization accuracy was quantified for the site of origin of the induced VT/PVC in millimeters, by comparing the predicted sites against the clinically defined locations.

Statistical Analysis

Mean and SD was used to report statistical analysis results. A comparison of the localization error between epicardial and endocardial VTs/PVCs was conducted using 2-sample *t*-test. A comparison of the localization error between VT exit sites and PVC origin sites

was conducted using 2-sample *t*-test. A double-sided $P < 0.05$ was considered statistically significant. Statistical analysis was performed with the Minitab 18 Statistical Software (Minitab Inc, State College, PA).

RESULTS

Patient Population

The baseline characteristics of the retrospective and prospective studies were summarized in Table 1. The retrospective study consisted of 19 patients (89.5% men, 66.6±9.1 years, 79% ischemic cardiomyopathy) with 21 LV VT ablation procedures. Two of 19 patients had 2 procedures: 1 was a standard VT ablation procedure, the other was a needle VT ablation procedure.⁶ Twenty-five out of 48 induced VTs had clinically identified VT exit sites and were used in the retrospective analysis.

The prospective study enrolled 23 patients (91.3% men, 62.7±18.3 years) with SHD. Patients in this case series underwent 5 epicardial and endocardial procedure, 3 epicardial only, and 15 endocardial only ablation procedures. A total of 49 induced VTs and PVCs were recorded by the AAOL system (Table 2). Twenty-six exit sites/site of origins of the induced 49 VTs and PVCs were clinically identified, and were used in the prospective analysis (Table 3).

Localization Accuracy of AAOL-Predicted Ventricular Arrhythmia Sites in the Retrospective Case Series Study

In the retrospective study, each procedure had 2.3±1.8 inducible VTs; 15.2±9.1 pacing sites were recorded. The 25 induced VTs were successfully localized onto the patient-specific EAM surface using the AAOL system. The localization error for the 25 VT exit sites using the AAOL system was 6.5±0.5 mm (mean±SE and an SD of 2.6 mm).

Table 3. Accuracy of the AAOL System for Localization of VT/PVC SoO and Pacing Sites From the Prospective Case Series Study

Case #	No. of pacing sites	Mean localization error of pacing sites (mm)	VT/PVC	VT exit/PVC origin/Ablation site	VT/PVC localization error (mm)
1	15	3.4±2.3	VT1	Basal inferoseptal wall of the LV endocardium	6.5
2	12	5.7±3.7	VT1	Basal anterolateral LV endocardium	6.0
	(12+20)*		VT2	Basal inferior LV endocardium	6.3
3	16	8.6±5.5	PVC1	Epicardial RV apex	6.9
			PVC2	Epicardial free wall of the RVOT	0.0
			PVC3	Epicardial basal inferior RV	7.7
4	15	5.3±3.9	VT1	Epicardial LV lateral wall	5.9
5	16	5.4±3.1	VT1	Lateral wall of the LV endocardium involving the anterolateral papillary muscle	5.5
6	12	5.5±3.4	VT1	†	...
			VT2	†	...
			VT3	†	...
7	13	3.5±2.0	VT1	‡	...
			VT2	§	...
8	15	6.2±4.5	VT1	§	...
			VT2	Basal inferior septum of the LV endocardium	10.6
			VT3	§	...
9	17	6.1±2.8	VT1	Inferior wall back to the annulus	7.0
			VT2	Lateral wall	6.3
10	10	5.3±2.8	VT1	Lateral RVOT of the RV endocardium	5.9
11	12	5.0±3.7	VT1	‡	...
			VT2	§	...
			VT3	‡	...
12	7	4.8±2.7
13	7 LV+3 RV	8.8±9.8	VT1	Mid-basal anteroseptal wall of the RV endocardium	1.9
14	15	5.4±3.6	PVC1	Epicardial anterolateral RV below RVOT	5.8
15	28	4.1±2.4	VT1	Low anteroseptal RVOT of the the RV endocardium	4.5
	9		VT2	LVOT area below LCC and LCC/RCC commissure of the LV endocardium	2.6
			VT3	§	...
16	8	3.7±2.1	VT1	Suggesting possibility of an epicardial/septal exit [†]	...
			VT2	‡	...
			VT3	Suggesting an epicardial exit [†]	...
17	20	6.2±3.3	VT1	Apical inferoseptal area of the LV endocardium	7.5
			VT2	Apical septal area of the LV endocardium	3.9
			VT3	‡	...
18	17	6.7±3.8	PVC1	Epicardial RVOT	2.0
			PVC2	Epicardial RV inferolateral wall	11.9

(Continued)

Table 3. Continued

Case #	No. of pacing sites	Mean localization error of pacing sites (mm)	VT/PVC	VT exit/PVC origin/Ablation site	VT/PVC localization error (mm)
19	10	7.5±3.1	VT1	§	...
			VT2	§	...
			VT3	§	...
20	28	4.5±3.7	VT1	‡	...
			VT2	Basal anterolateral wall of the LV endocardium	6.5
			VT3	‡	...
			VT4	Mid inferior septum of the LV endocardium	4.5
			VT5	‡	...
			VT6	‡	...
21	11	6.1±3.4	VT1	Basal lateral LV wall	3.9
	(11+7)*		VT2	Basal and anterior lateral LV wall	8.3
22	9	6.7±2.8	VT1	Epicardial apical inferolateral LV wall	8.2
23	7	3.2±3.7	VT1	‡	...
			VT2	Basal inferior septum of the LV endocardium	6.7

The localization errors of ventricular tachycardia (VT)/premature ventricular contraction SoO localization and pacing sites were calculated as Euclidean distance between the estimated site and the known site/clinically identified site. LV indicates left ventricular; LVOT, left ventricular outflow tract; PVC, premature ventricular contraction; RV, right ventricular; RVOT, right ventricular outflow tract.

*Defines a set of pacing sites that consists of previous pacing sites from mapping VT1 and the recorded additional pacing sites from mapping VT2.

†VTs that were terminated within the middle of the scar at sites proximal to the scar exit site (in which cases localization accuracy could not be precisely quantitated because VT was terminated at a mid-diastolic site).

‡VT was not mapped, and an exit site was therefore not identified.

§Site of origin/ablation site was only approximately localized.

Localization Accuracy of the AAOL-Predicted Pacing Sites in the Prospective Case Series Study

Localization accuracy was tested for all 359 recorded pacing sites in the prospective study with a mean 15.6±7.7 pacing sites per patient. The AAOL system achieved a mean localization accuracy of 5.5±3.9 mm for the pooled pacing sites. For each patient, the mean value and SD of the localization error of the AAOL for recorded pacing sites are shown in Table 3. The AAOL system had a mean 5.6±0.3 mm (mean±SE) and an SD of 1.5 mm over all 23 patients. Figure 1 presents the localization accuracy of the recorded pacing sites for each patient using the AAOL system.

Localization Accuracy of the AAOL-Predicted VT Exit/PVC Origin Site in the Prospective Case Series Study

Patients had 2.1±1.3 VTs/PVCs. The 26 inducible VT and PVC morphologies (8 epicardium and 18 endocardium) with clinically confirmed exit or origin sites were successfully localized onto the patient-specific EAM surface using the AAOL system. The mean localization

accuracy was 5.9±0.5 mm (mean±SE) and an SD of 2.6 mm for the 26 VT exit and PVC origin sites, which is summarized in Figure 2. In the prospective case series study, there was no difference in mean localization error for epicardial compared with endocardial sites using the AAOL (6.0 versus 5.8 mm, *P*=0.895); the VT exit site and PVC origin site predictions had similar localization performance using the AAOL system (6.0 versus 5.5 mm, *P*=0.782).

Examples of VT Exit Site Localization

Below we describe 3 representative cases to illustrate the ability of the AAOL system to localize PVC origin/VT exit sites from epicardial and endocardial anatomical locations. Details of the AAOL used practically were presented in online supplementary materials.

Patient #3; Arrhythmogenic Right Ventricular Cardiomyopathy

The first clinical PVC had a left bundle branch block-type morphology, superior axis, and negative concordance in all precordial leads (Figure 3A). Epicardial EAM surface mesh was created using the EnSite mapping system. Pace mapping and activation mapping

was performed; and the PVC origin site was identified on the epicardial RV apex clinically and was indicated by a yellow star on the EAM map (Figure 3B). Radiofrequency ablation lesions were applied over this area, resulting in suppression of the PVC. Figure 3C shows that the AAOL system predicted accurately the site of the PVC origin on the epicardial RV apex, achieving a localization accuracy of 6.9 mm when using all recorded pacing sites (n=16). The second clinical PVC had a left bundle branch block-type morphology with an inferior axis, and a precordial lead transition at V3 (Figure 3D). Activation mapping and pace mapping of the PVC was performed; the PVC was targeted on the epicardial right ventricular outflow tract indicated by the yellow star (Figure 3E). The AAOL system achieved a localization error of 0.0 mm, in comparison with the red star site identified clinically (Figure 3F). The third clinical PVC had a left bundle branch block-type morphology with a superior axis, and a transition in the precordial lead at V4 (Figure 3G). The PVC was targeted by pace mapping and activation mapping to the RV basal inferior wall as shown in Figure 3H. Radiofrequency ablation here resulted in suppression of the PVC. The AAOL system predicted the site of PVC origin onto the epicardial RV basal inferior wall, having a localization error of 7.7 mm, as shown in Figure 3I.

Patient #13; Ischemic Cardiomyopathy

The VT had a left bundle branch block-type morphology, a left inferior axis, a precordial lead transition at V3 and cycle length 281 ms (Figure 4A). During the procedure, significant endocardial scar was revealed, with local abnormal ventricular activity and late potentials in the apex, apical lateral, mid-lateral and basal lateral-anterolateral wall of the left ventricle. There were poor correlations between paced QRS morphologies and the induced VT in the LV. Seven pacing sites were collected from the LV endocardium. Using the 7 pacing sites and the AAOL software, the VT exit site was localized outside of the LV endocardial EAM geometry, suggesting an RV exit site (Figure 4C). An RV endocardial EAM map was created using a multipolar (Penta-Ray) catheter; pace-mapping was performed at the mid-basal anteroseptal wall of RV, yielding a pace-mapping site with 88% PaSo score (calculated by PaSo module, Carto 3 system, Biosense Webster, Diamond Bar, CA) as the clinically-identified VT exit site (Figure 4B, yellow star). We recorded 3 more RV pacing sites and used the 10 pacing-site data to localize a VT exit site onto the mid-basal anteroseptal wall of RV, achieving a localization accuracy within 2.0 mm after including both RV and LV endocardial geometries, as shown in Figure 4D.

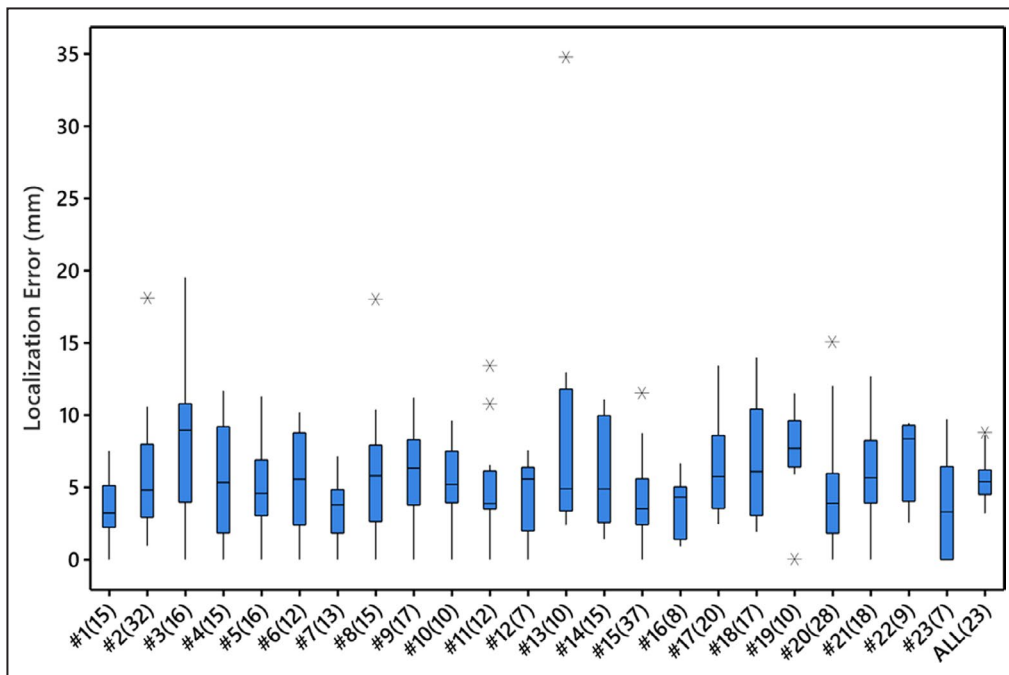


Figure 1. Error in localizing the recorded pacing sites of each patient and a mean patient localization error by the automatic arrhythmia-origin localization system in the prospective case series study.

Boxes represent interquartile ranges; error bars represent the ranges for the bottom 25% and the top 25% of the data values, excluding outliers; line in the box indicates median and “*” represents outliers located outside the whiskers of the box plot. The ALL(23) plot represents the mean of the mean localization errors over all 23 patients. Sample sizes are included in parentheses brackets.

Patient #22; Ischemic Cardiomyopathy

The VT had cycle length 400 ms, with right bundle branch block-type morphology in lead V1, and an indeterminate axis with negative in II and positive in lead III (Figure 5A). Pace-mapping was performed epicardially, near the apical inferior margin of the inferolateral scar, yielding sites with perfect pace matches and Stim-QRS >40 msec. The VT exit site was clinically identified by pace-mapping before termination of VT by radiofrequency application (Figure 4B, yellow star). Using the AAOL, the VT exit site was localized to the epicardial apical inferolateral LV wall, achieving a localization accuracy of 8.2 mm after using data acquired from 9 pacing sites. Figure 4C shows the clinically identified VT exit site indicated by the red star and on the corresponding estimated VT exit site marked by a blue patch on the epicardial EAM surface.

DISCUSSION

In this study of 2 case series studies of patients with structural heart disease presenting for catheter ablation for ventricular arrhythmias, we demonstrated that

(1) it is feasible to use the AAOL system to localize VT exit/PVC origin sites on both the epicardial and endocardial EAM surface; (2) the AAOL system, tested using 2 commercially available mapping systems (Carto 3 and EnSite TM Precision mapping systems), identifies VT exit/PVC origin sites with a mean localization error of 6.5 mm in the retrospective study and 5.9 mm in the prospective study. The AAOL system achieves data collection and localization analysis in real time and uses pacing data during the ablation procedure to localize VT exit/PVC origin sites onto intracardiac EAM surfaces. In addition, there was not much difference in localization accuracy between VT exit and PVC origin sites, indicating that the AAOL algorithm performs equally well in both cases. The reason for this is that anatomical and functional complexities around VT exit sites in SHD, manifested in substrate mapping or high-resolution imaging modality, do not play a role in the algorithm, which relies only on information about ECGs from known pacing sites.

Several automatic ECG-based localization approaches have been developed to identify VT exit/PVC origin sites. Li et al presented a navigation algorithm based on pace mapping for locating the exit

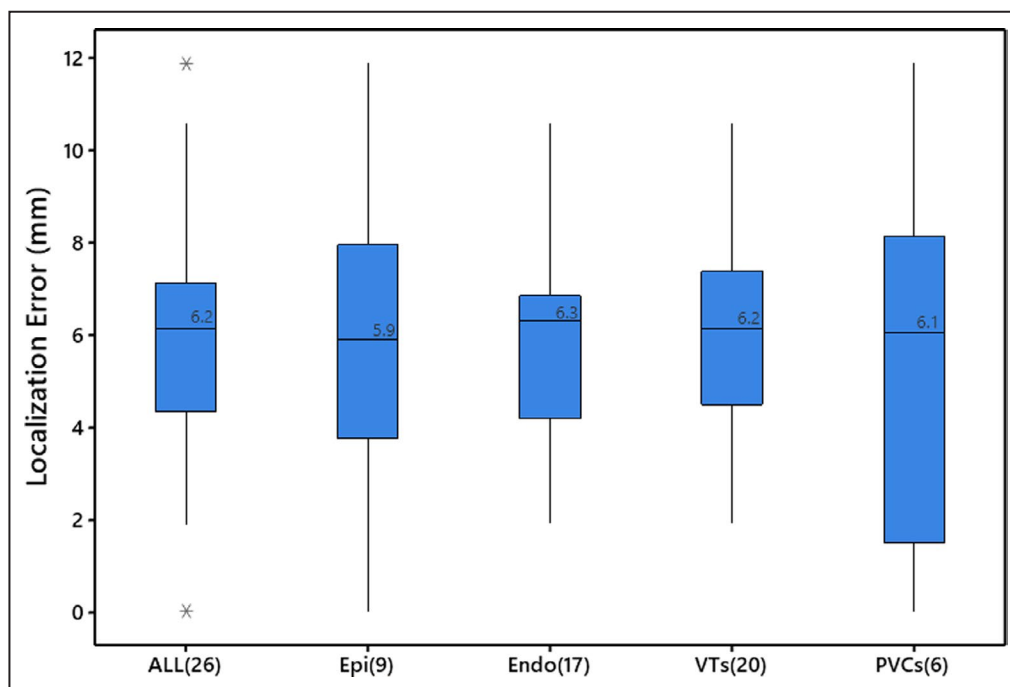


Figure 2. Box plot of localization errors between clinically identified ventricular tachycardia exit/premature ventricular contraction origin sites and sites estimated by the automatic arrhythmia-origin localization system in the prospective case series study.

Boxes represent interquartile ranges; error bars represent the ranges for the bottom 25% and the top 25% of the data values, excluding outliers; “*” indicates outliers located outside the whiskers of the box plot; line and value in the box indicate the median value. The ALL plot represents the aggregate of all ventricular tachycardias and premature ventricular contractions. Endo indicates endocardial ventricular tachycardias and premature ventricular contractions; Epi, epicardial ventricular tachycardias and premature ventricular contractions; PVC, premature ventricular contractions; and VT, ventricular tachycardias. Sample sizes are included in parentheses brackets.

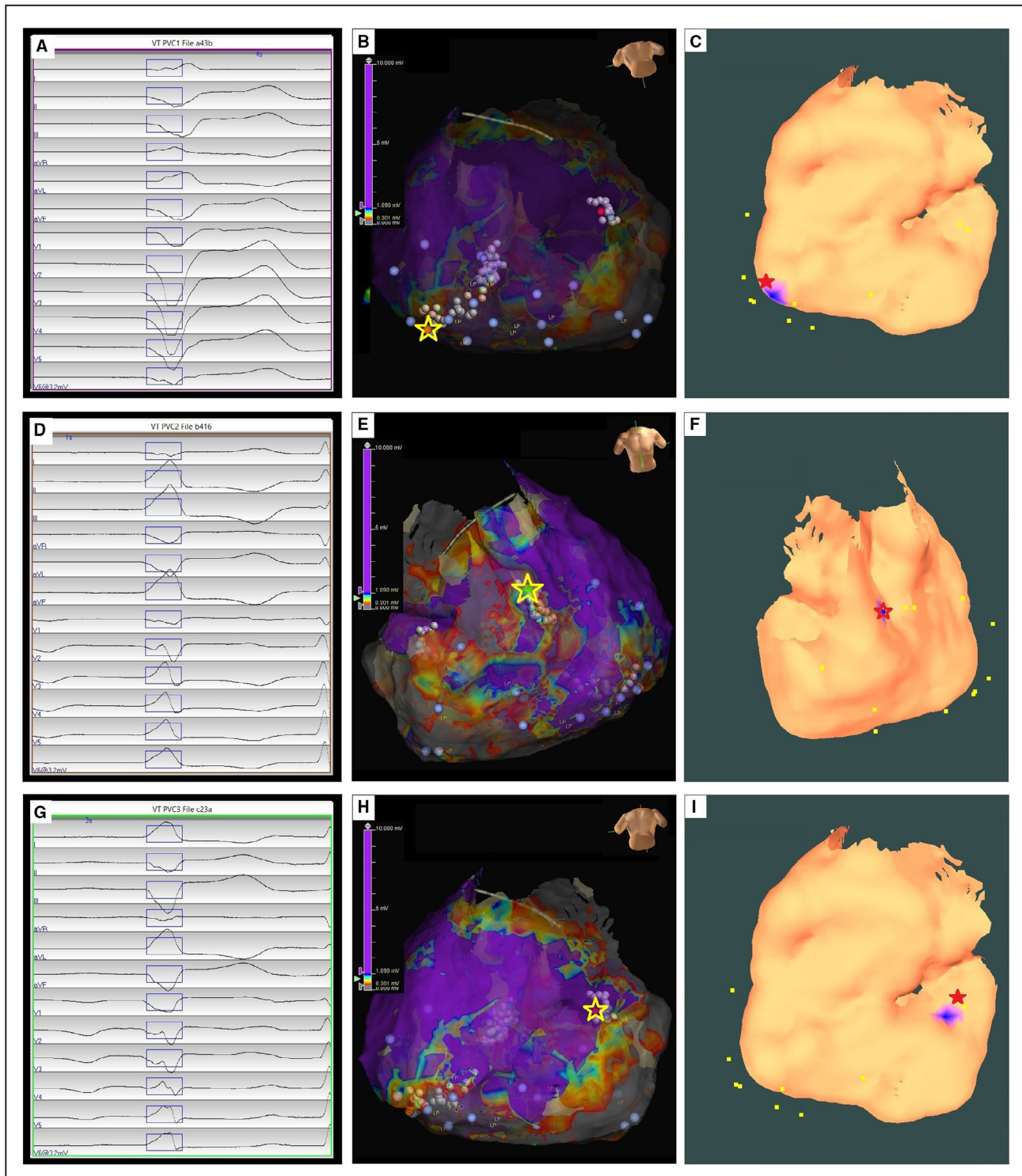


Figure 3. Localization of 3 premature ventricular contraction (PVC)-origin sites by the automatic arrhythmia-origin localization system.

A, D, G, Recorded 12-lead ECG of PVCs during the procedure for a patient with arrhythmogenic right ventricular cardiomyopathy. **B, E, H,** Epicardial substrate map for this patient, with the PVC-origin site (identified by activation and pace mapping) depicted by the yellow star. **C, F, I,** Usage of the automatic arrhythmia-origin localization system to predict a PVC origin site indicated by the blue patch onto the epicardial electroanatomic mapping surface, with the actual site of PVC origin marked by the red star.

site of VA within a median area of 196.5 mm² in patients with and without SHD. Although the navigation algorithm demonstrated the feasibility of identifying a target region for navigating to the next pacing site, it depends on the operator's experience for collecting pacing sites within the neighborhood of the site of origin of the induced VTs.¹⁷ Alawad and Wang proposed a patient-specific regression model to localize the origin of VA onto 1 of 26 segments of the ventricles, achieving an \approx 400 mm² resolution.¹⁸ He et al presented a data-driven approach based on an automatic beat recognition algorithm to localize the PVC origin to 11 regions of the entire ventricle,¹⁹ with a localization accuracy of 70.7% to 74.7%. Gyawali et al presented a deep-learning based model trained on the ECG of 1012 known pacing sites to localize the origin of LV activation site; however, this classification was into just 10 LV segments.²⁰ We have previously shown that the AAOL system obtains small localization errors (mean 3.6 mm) for diverse focal VA locations⁷ and this study further extends the clinical applicability by demonstrating accurate localization of VT exit/PVC origin sites in patients with structural heart disease. The advantage of this system, compared with other published non-invasive ECG localization systems discussed above, is the ability to achieve real-time precise localization on the clinical intracardiac patient-specific EAM using only 3-lead ECGs (leads III, V2, V6) and pacing sites.

Rapid, accurate localization of VT exit/PVC origin sites can be helpful in planning and potentially improving the efficacy of catheter ablation of ventricular arrhythmias.

The majority of patients have at least 1 VT which cannot be specifically mapped, and for which a clear single culprit site cannot be identified. Unmappable VT can be approached with the use of 3-dimensional voltage mapping of the culprit substrate, and targeted ablation of tissue with abnormal signals, which are typically located within diseased myocardial tissue. Some have advocated for ablation of the entire scar in the hopes of destroying any potential arrhythmogenic substrate, although a broader ablation approach such as this may carry the risk of insufficient focus on highest value substrate. A common method for the identification of sites likely to participate in clinically relevant VTs is to create a 3-dimensional map of the arrhythmogenic substrate, induce VT, and identify portions of the scar which harbor exit sites. This depends upon rapid interpretation of the 12-lead ECG, combined with pace-mapping to identify areas which match the morphology of the induced VT. Efforts may then be focused with greater specificity on ablating the sites within the scar which are contiguous with the exit site. The AAOL system, which can accurately localize a region containing a VT exit/PVC origin site, can potentially reduce the time needed for detailed mapping by quickly identifying a focused region of interest.

Limitations

The overall study size is small (n=42); however, the system was validated using data from 2 centers and in a diverse study of VT locations. While this is a pilot study, we nonetheless did test the localization accuracy of

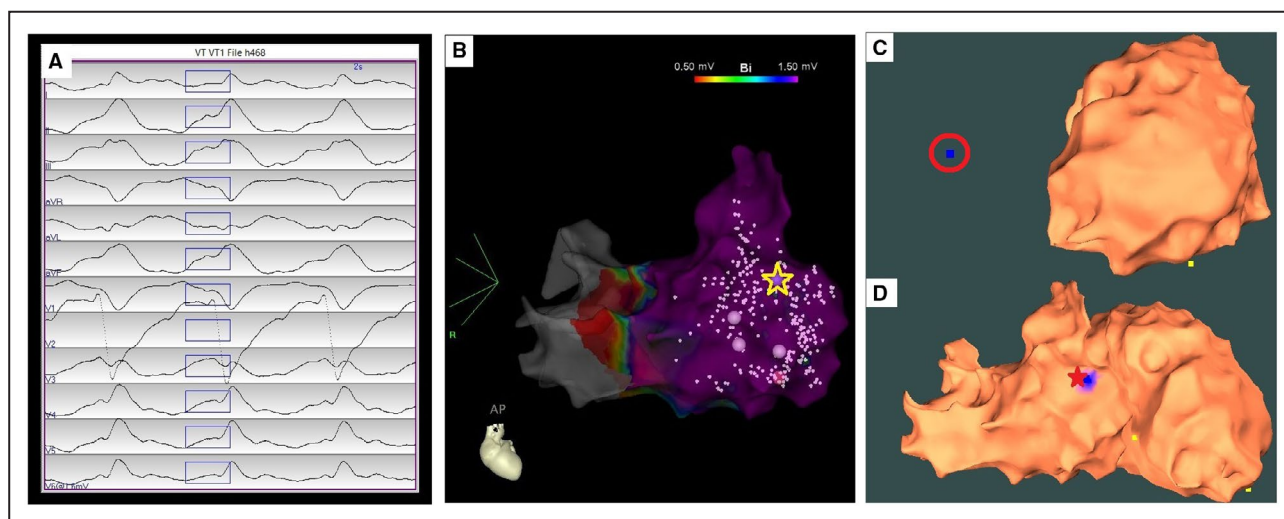


Figure 4. Localization of a ventricular tachycardia (VT) exit site on the right ventricular electroanatomic mapping (EAM) surface by the automatic arrhythmia-origin localization system.

A, Recorded 12-lead ECG of an induced VT during the procedure for patient #13. **B**, Patient-specific right ventricular EAM with antero-posterior view, with the VT exit site (identified by pace-mapping) depicted by the yellow star. **C**, Usage of the automatic arrhythmia-origin localization system to predict a VT exit site indicated by the blue dot with a red circle outside of the left ventricular EAM geometry when mapping at the left ventricle. **D**, The automatic arrhythmia-origin localization system was used to predict the VT exit site marked in the blue patch onto the mid-basal antero-septal wall of right ventricle after including the right ventricular EAM geometry, achieving a localization accuracy of 1.9 mm. The actual VT exit site marked by the red star; yellow dots indicate recorded pacing sites on the EAM.

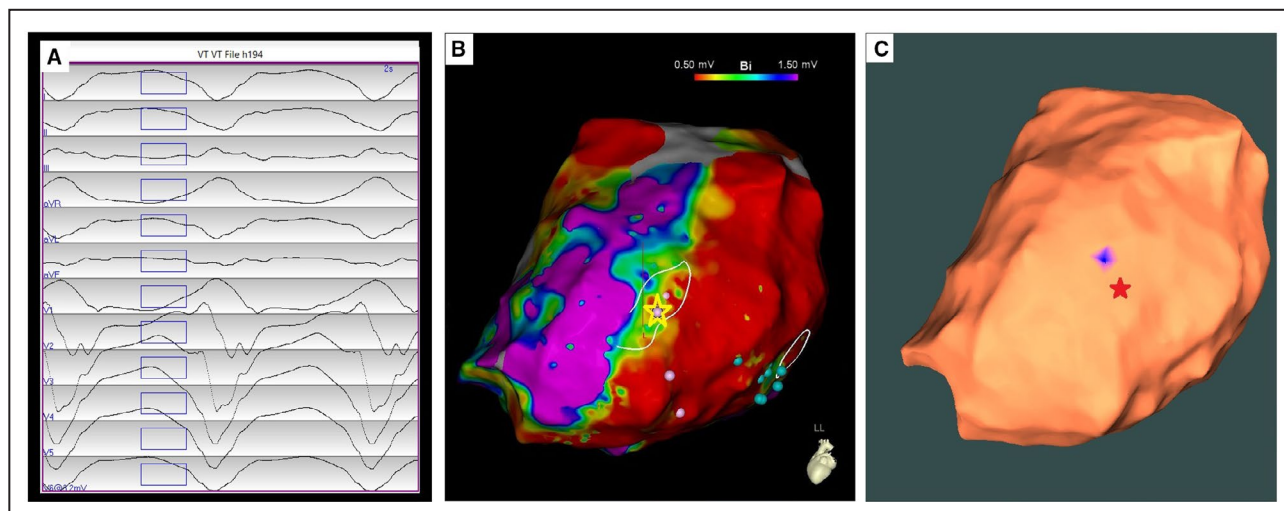


Figure 5. Localization of an epicardial ventricular tachycardia (VT) exit site by the automatic arrhythmia-origin localization system.

A, Recorded 12-lead ECG of an induced epicardial VT during the procedure for patient #22. **B**, Epicardial electroanatomic mapping bipolar potential map of the left ventricle for this patient, with the VT exit site (identified by contact mapping) depicted by the yellow star. **C**, The automatic arrhythmia-origin localization system was used to predict a VT exit site marked in the blue patch on the apical inferolateral left ventricular wall of the epicardial electroanatomic mapping geometry when using all recorded 9 pacing sites of the VT, having a localization error of 8.2 mm in comparison with the actual VT exit site indicated by the red star.

the AAOL system on 2 commercial mapping systems (Ensite and Carto), illustrating the system's versatility. Further, the localization error range is small for VT exit locations. As this is a pilot study, the numerous advantages of the AAOL system point towards an improved and potentially faster clinical targeting during the clinical ablation procedure. We cannot demonstrate that quantitatively in this pilot study, as the AAOL system needs to be integrated into an existing EAM system to assess its performance in the field. It is worth nothing that the AAOL approach can identify the site of activation of ventricular myocardium; this may not be an ideal site for ablation but rather a guide for further substrate analysis.

CONCLUSIONS

The study retrospectively and prospectively assessed the accuracy of the AAOL system for localizing the VT exit/PVC origin site in both endocardial and epicardial ventricles. The localization performance was promising, and thus, AAOL system could potentially facilitate ablation procedures for patients with SHD.

ARTICLE INFORMATION

Received May 25, 2021; accepted August 25, 2021.

Affiliations

Alliance for Cardiovascular Diagnostic and Treatment Innovation, Johns Hopkins University, Baltimore, MD (S.Z., E.S., R.B., H.T., N.A.T., J.C.); Department of Medicine, Queen Elizabeth II Health Sciences Centre, Halifax, NS, Canada (A.A., J.L.S.); Division of Cardiology, Department of Medicine, Section of Cardiac Electrophysiology, Johns Hopkins Hospital, Baltimore, MD (K.N.A., R.S., R.B., H.T., J.C.); Department of Physiology and Biophysics (J.L.S.,

J.W.W., P.J.M.) and School of Biomedical Engineering (B.M.H.), Dalhousie University, Halifax, NS, Canada; and Department of Biomedical Engineering, Johns Hopkins University, Baltimore, MD (E.S., K.N.A., N.A.T.).

Sources of Funding

This work was supported by funding support from Heart Rhythm Society Postdoctoral Fellowship to S.Z.; Department of Medicine of Dalhousie University to A.A., Maritime Heart Centre grant to A.A.; National Institutes of Health [R01HL142496 and R01HL126802] to N.T., Leducq 16CVD02 to N.T.; Robert E. Meyerhoff Professorship to J.C.

Disclosures

Drs Zhou, Trayanova, Chrispin, AbdelWahab, and Sapp report a patent to Intraprocedural Automated System for Localizing Idiopathic Ventricular Arrhythmia Origins pending. Dr John L. Sapp reports grants from Biosense Webster, grants from Abbott, personal fees from Biosense Webster, personal fees from Medtronic, and personal fees from Abbott outside the submitted work; in addition, Dr Sapp has a patent to Needle Ablation Catheter issued and a patent to ECG Localization Software issued. Dr B. Milan Horáček is a co-holder of a patent for automated VT localization; no licensing, royalties or income currently or anticipated. Dr Amir AbdelWahab reports speaker honoraria from Abbott and Medtronic. Dr Harikrishna Tandri reports grants from Abbott outside the submitted work. The remaining authors have no disclosures to report.

REFERENCES

- Sapp JL, Wells GA, Parkash R, Stevenson WG, Blier L, Sarrazin JF, Thibault B, Rivard L, Gula L, Leong-Sit P, et al. Ventricular tachycardia ablation versus escalation of antiarrhythmic drugs. *N Engl J Med*. 2016;375:111–121. doi: 10.1056/NEJMoa1513614
- Miller JM, Marchlinski FE, Buxton AE, Josephson ME. Relationship between the 12-lead electrocardiogram during ventricular tachycardia and endocardial site of origin in patients with coronary artery disease. *Circulation*. 1988;77:759–766. doi: 10.1161/01.CIR.77.4.759
- Yokokawa M, Liu T, Yoshida K, Scott C, Hero A, Good E, Morady F, Bogun F. Automated analysis of the 12-lead electrocardiogram to identify the exit site of postinfarction ventricular tachycardia. *Heart Rhythm*. 2012;9:330–334. doi: 10.1016/j.hrthm.2011.10.014
- Sapp JL, Bar-Tal M, Howes AJ, Toma JE, El-Damaty A, Warren JW, MacInnis PJ, Zhou S, Horáček BM. Real-time localization of ventricular

- tachycardia origin from the 12-lead electrocardiogram. *JACC Clin Electrophysiol.* 2017;3:687–699. doi: 10.1016/j.jacep.2017.02.024
5. Zhou S, AbdelWahab A, Sapp JL, Warren JW, Horáček BM. Localization of ventricular activation origin from the 12-Lead ECG: a comparison of linear regression with non-linear methods of machine learning. *Ann Biomed Eng.* 2019;47:403–412. doi: 10.1007/s10439-018-02168-y
 6. Zhou S, AbdelWahab A, Horáček BM, MacInnis PJ, Warren JW, Davis JS, Elsokkari I, Lee DC, MacIntyre CJ, Parkash R, et al. Prospective assessment of an automated intraprocedural 12-lead ECG-based system for localization of early left ventricular activation. *Circ Arrhythm Electrophysiol.* 2020;13:e008262. doi: 10.1161/CIRCEP.119.008262
 7. Zhou S, AbdelWahab A, Sapp JL, Sung E, Aronis KN, Warren JW, MacInnis PJ, Shah R, Horáček BM, Berger R, et al. Prospective multi-center assessment of a new intraprocedural automated system for localizing idiopathic ventricular arrhythmia origins. *JACC Clin Electrophysiol.* 2021;7:395–407. doi: 10.1016/j.jacep.2020.09.009
 8. Pathak RK, Ariyaratna N, Garcia FC, Sanders P, Marchlinski FE. Catheter ablation of idiopathic ventricular arrhythmias. *Heart Lung Circ.* 2019;28:102–209. doi: 10.1016/j.hlc.2018.10.012
 9. Stevenson WG, Tedrow UB, Reddy V, AbdelWahab A, Dukkipati S, John RM, Fujii A, Schaeffer B, Tanigawa S, Elsokkari I, et al. Infusion needle radiofrequency ablation for treatment of refractory ventricular arrhythmias. *J Am Coll Cardiol.* 2019;73:1413–1425. doi: 10.1016/j.jacc.2018.12.070
 10. Sosa E, Scanavacca M, d'Avila A. Gaining access to the pericardial space. *Am J Cardiol.* 2002;90:203–204. doi: 10.1016/S0002-9149(02)02426-8
 11. Keramati AR, DeMazumder D, Misra S, Chrispin J, Assis FR, Raghuram C, Dey S, Calkins H, Tandri H. Anterior pericardial access to facilitate electrophysiology study and catheter ablation of ventricular arrhythmias: a single tertiary center experience. *J Cardiovasc Electrophysiol.* 2017;28:1189–1195. doi: 10.1111/jce.13296
 12. Stevenson WG, Friedman PL, Sager PT, Saxon LA, Kocovic D, Harada T, Wiener I, Khan H. Exploring postinfarction reentrant ventricular tachycardia with entrainment mapping. *J Am Coll Cardiol.* 1997;29:1180–1189. doi: 10.1016/S0735-1097(97)00065-X
 13. Dixit S, Callans DJ. Mapping for ventricular tachycardia. *Card Electrophysiol Rev.* 2002;6:436–441.
 14. Stevenson WG, Friedman PL, Kocovic D, Sager PT, Saxon LA, Pavri B. Radiofrequency catheter ablation of ventricular tachycardia after myocardial infarction. *Circulation.* 1998;98:308–314. doi: 10.1161/01.CIR.98.4.308
 15. Bogun F, Good E, Reich S, Elmouchi D, Igic P, Lemola K, Tschopp D, Jongnarangsin K, Oral H, Chugh A, et al. Isolated potentials during sinus rhythm and pace-mapping within scars as guides for ablation of post-infarction ventricular tachycardia. *J Am Coll Cardiol.* 2006;47:2013–2019. doi: 10.1016/j.jacc.2005.12.062
 16. Soejima K, Stevenson WG, Maisel WH, Sapp JL, Epstein LM. Electrically unexcitable scar mapping based on pacing threshold for identification of the reentry circuit isthmus: feasibility for guiding ventricular tachycardia ablation. *Circulation.* 2002;106:1678–1683. doi: 10.1161/01.CIR.0000030187.39852.A7
 17. Li A, Davis JS, Grimster A, Wierwille J, Herold K, Morgan D, Behr ER, Shorofsky S, Saba M. Proof of concept study of a novel pacemap algorithm as a basis to guide ablation of ventricular arrhythmias. *Europace.* 2018;20:1647–1656. doi: 10.1093/europace/euy024
 18. Alawad M, Wang L. Learning domain shift in simulated and clinical data: localizing the origin of ventricular activation from 12-lead electrocardiograms. *IEEE Trans Med Imaging.* 2019;38:1172–1184. doi: 10.1109/TMI.2018.2880092
 19. He K, Nie Z, Zhong G, Yang C, Sun J. Localization of origins of premature ventricular contraction in the whole ventricle based on machine learning and automatic beat recognition from 12-lead ECG. *Physiol Meas.* 2020;41:055007. doi: 10.1088/1361-6579/ab86d7
 20. Gyawali PK, Horáček BM, Sapp JL, Wang L. Sequential factorized autoencoder for localizing the origin of ventricular activation from 12-lead electrocardiograms. *IEEE Trans Biomed Eng.* 2020;67:1505–1516.